

Phase Change Materials for Thermal Management of IC Packages

Ivo BĚHUNEK, Pavel FIALA

Dept. of Theoretical and Experimental Electrical Engineering, Brno University of Technology,
Kolejní 4, 612 00 Brno, Czech Republic

behunek@feec.vutbr.cz, fialap@feec.vutbr.cz

Abstract. This paper deals with the application of phase change materials (PCM) for thermal management of integrated circuits as a viable alternative to active forced convection cooling systems.

The paper presents an analytical description and solution of heat transfer, melting and freezing process in 1D which is applied to inorganic crystalline salts. There are also results of numerical simulation of a real 3D model. These results were obtained by means of the finite element method (FEM). Results of 3D numerical solutions were verified experimentally.

Keywords

Phase change, FEM, heat, integrated circuit.

1. Introduction

Phase change materials can store large amounts of heat without undergoing significant temperature changes because of their high latent heat of fusion. There are known the following basic PCM classification [9]

1) Inorganic

Advantages – high latent heat, good thermal conductivity, non-flammable, cheap

Disadvantages – corrosive effect on most metals, phase decomposition and loss of hydrate, supercooling
Examples – $\text{CaCl}_2 \cdot 6\text{H}_2\text{O}$, $\text{Na}_2\text{SO}_4 \cdot 10\text{H}_2\text{O}$ etc.

2) Organic

Advantages – high latent heat, chemically stable, little or no supercooling, cheap, non-corrosive, non-toxic

Disadvantages – low thermal conductivity, big volume changes during phase change, flammability
Examples – paraffin wax, polyethylenglycol, high-density polyethylene, stearic acid ($\text{C}_{18}\text{H}_{36}\text{O}_2$), palmitic acid ($\text{C}_{16}\text{H}_{32}\text{O}_2$) etc.

3) Compounds, combinations of amorphous and crystalline substances, clathrates etc.

The amounts of stored energy are given by the calorimetric equation

$$Q = \rho V \Delta h_m + \int_{T_0}^{T_m} V \rho c dT + \int_{T_m}^{T_e} V \rho c dT \quad (1)$$

where ρ is the density, V the volume, c the specific heat, Δh_m the specific enthalpy, Q the heat, T_0 , T_m , T_e , the initial, phase change and the final temperature of inorganic compounds during the accumulation process (see Fig. 1).

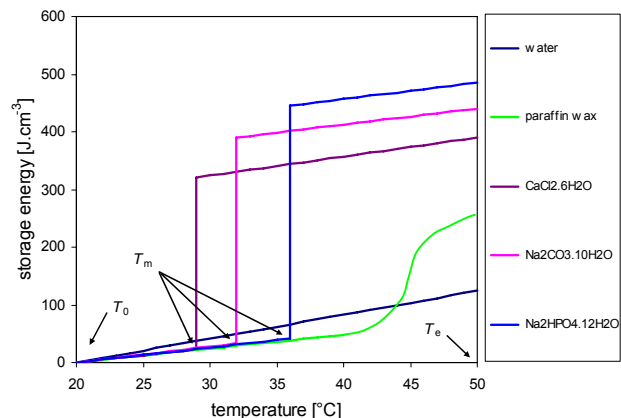


Fig. 1. Heating process of different PCMs and water (density of stored energy).

The PCM may be used for active or passive electronic cooling applications with high power at the package level (see [1]).

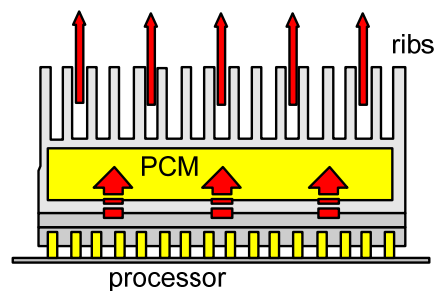


Fig. 2. Example of processor cooler with phase change material.

2. Analytical Description and Solution of Heat Transfer and Phase Change

We deal with the problem of heat transfer in 1D body during melting and freezing process with an external heat flux or heat convection, which is given by boundary conditions. The solution of this problem is known (Neumann, 1864) for solidification of metals [10]. We tried to apply this theory to melting of crystalline salts. The 1D body could be a semifinite plane, cylinder or sphere [3]. As the solid and the liquid part of PCM have different temperatures, there is a heat transfer on the interface. According to Fig. 3 the origin of x is the axis of pipe, centre of sphere or the origin of plate. Liquid starts to solidify if the surface is cooled by flowing fluid ($T_w < T_m$).

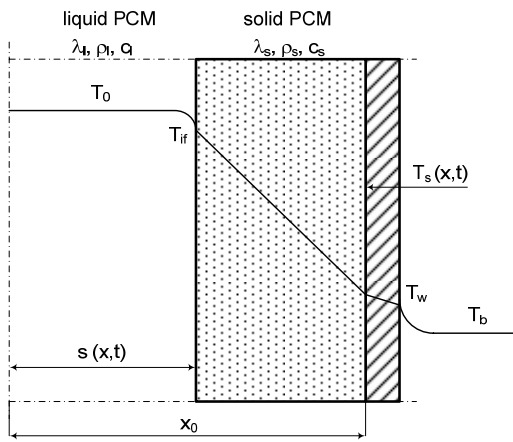


Fig. 3. Heat transfer on the interface between the solid and the liquid parts.

The equation describing the solid state is

$$\frac{\partial T_s}{\partial t} = \frac{a_s}{x^n} \frac{\partial}{\partial x} \left(x^n \frac{\partial T_s}{\partial x} \right) \quad (2)$$

where for the plate $n = 0$, cylinder $n = 1$ and sphere $n = 2$, a_s is the thermal diffusion coefficient in the solid state. For $x = x_0$ we can assume these boundary conditions

constant temperature

$$T = T_w \quad (3)$$

or constant heat flux

$$\lambda_s \frac{\partial T_s}{\partial x} = -q_w \quad (4)$$

or for convective cooling

$$\lambda_s = \frac{\partial T_s}{\partial x} = -k(T - T_b) \quad (5)$$

where q_w is the specific heat flux and λ_s is the thermal conductivity coefficient. The initial condition ($t = 0$) for (2) is

$$T_s(0) = T_0. \quad (6)$$

For the interface between the solid and the liquid we obtain

$$\rho_s \Delta h_m \frac{ds}{dt} = \lambda_s \frac{\partial T_s}{\partial x} + \alpha(T_m - T_0). \quad (7)$$

The analytical solution is exact but we consider several simplifying assumptions. The most important of them is that we can solve the solidification of PCM only in one dimensional body.

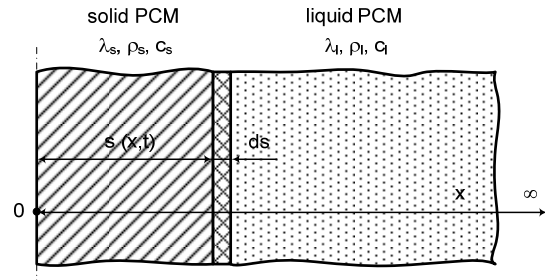


Fig. 4. Solidification of semi-infinite plate of PCM.

We consider semi-infinite mass of liquid PCM at the initial temperature T_0 which has been cooled by a sudden drop of surface temperature $T_p = 0^\circ\text{C}$. This temperature is constant during the whole process of solidification. The simplifying assumptions are

- body is semi-infinite plane
- heat flux is one-dimensional in the x -axis
- interface between the solid and the liquid is planar
- there is an ideal contact on the interface
- temperature of surface is constant ($T_p = 0^\circ\text{C}$)
- crystallization of PCM is at a constant temperature T_m
- thermophysical properties of the solid and the liquid are different but they do not depend on the temperature
- there is no natural convection in the liquid.

Initial and boundary conditions:

- the initial temperature T_0 for $x \geq 0$ at the time 0
- the temperature equals to T_m on the interface between the solid and the liquid ($x = s$)

$$x = s \wedge t > 0 \Rightarrow T_s = T_l = T_m = \text{const} \quad (8)$$

- evolved latent heat during a motion of interface (the thickness of volume element ds , area 1 m^2 , time 1 s)

$$dQ_{\Delta h_m} = \Delta h_m \rho_l 1 \frac{ds}{dt} \quad (9)$$

- the position of interface is a function of time

$$s = s(t) = 2\varepsilon \sqrt{a_s t}, \quad (10)$$

this dependence is called the parabolic law of solidification, where ε is the root of equation describing the freezing..

- the boundary and initial condition for phase change

$$\lambda_s \left(\frac{\partial T_s}{\partial x} \right)_{x=s} = \lambda_l \left(\frac{\partial T_l}{\partial x} \right)_{x=s} + \Delta h_m \rho_l \frac{ds}{dt} \quad (11)$$

$$x \rightarrow \infty \wedge t > 0 \Rightarrow T_l = T_0 = \text{const} \quad (12)$$

$$x = 0 \wedge t \geq 0 \Rightarrow T_p = T_s(x=0) = 0^\circ\text{C} \quad (13)$$

If we solve the Fourier relations of heat conduction with conditions above for the solid and the liquid, we get the following equations which allow calculating temperatures in solid, liquid PCM and the location of interface. The results are in figures 5-8 which are related to equations 10, 15, 16.

$$\frac{e^{-\varepsilon^2}}{\text{erf}(\varepsilon)} - \frac{\lambda_l}{\lambda_s} \sqrt{\frac{a_s}{a_l}} \frac{T_0 - T_m}{T_m} \frac{e^{-\frac{a_s \varepsilon^2}{a_l}}}{\text{erfc}\left(\varepsilon \sqrt{\frac{a_s}{a_l}}\right)} = \quad (14)$$

$$= \frac{\Delta h_m \rho_l \varepsilon a_s \sqrt{\pi}}{\lambda_s T_m}$$

We get $\varepsilon = 0.3514$ for $\text{CaCl}_2 \cdot 6\text{H}_2\text{O}$, $\varepsilon = 0.3257$ for $\text{Na}_2\text{CO}_3 \cdot 10\text{H}_2\text{O}$ and $\varepsilon = 0.3319$ for $\text{Na}_2\text{HPO}_4 \cdot 12\text{H}_2\text{O}$.

$$T_s = \frac{T_m}{\text{erf}(\varepsilon)} \text{erf}\left(\frac{x}{2\sqrt{a_s t}}\right) \quad (15)$$

$$T_l = T_0 + \frac{T_0 - T_m}{\text{erfc}\left(\varepsilon \sqrt{\frac{a_s}{a_l}}\right)} \text{erfc}\left(\frac{x}{2\sqrt{a_l t}}\right) \quad (16)$$

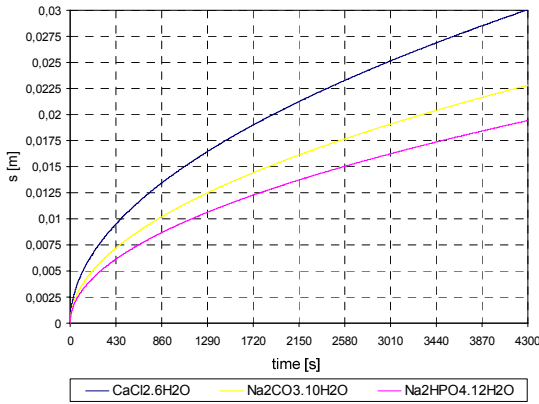


Fig. 5. Position between the solid and the liquid PCM.

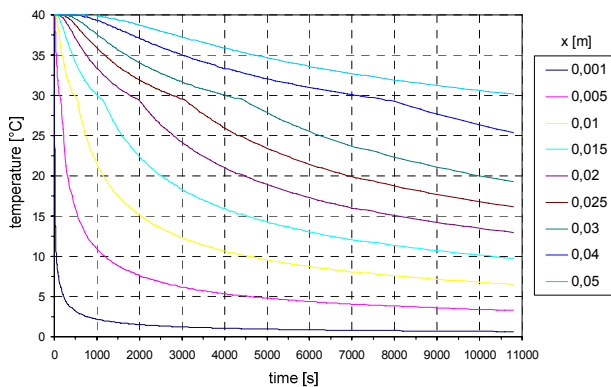


Fig. 6. Dependence of temperature on distance ($\text{CaCl}_2 \cdot 6\text{H}_2\text{O}$).

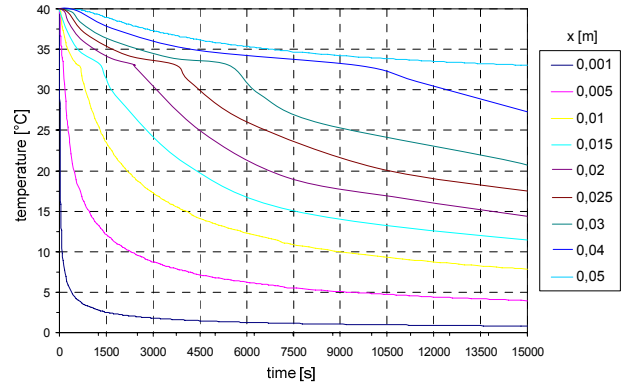


Fig. 7. Dependence of temp. on distance ($\text{Na}_2\text{CO}_3 \cdot 10\text{H}_2\text{O}$).

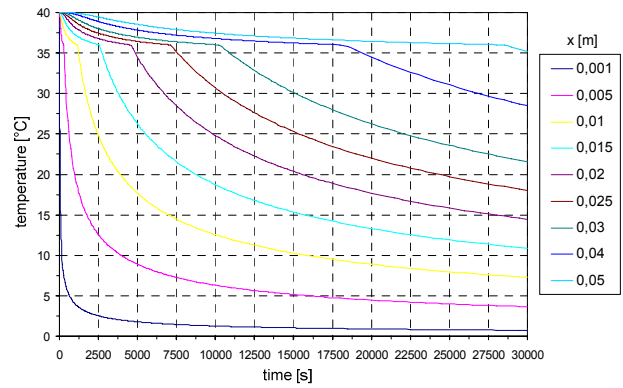


Fig. 8. Dependence of temp. on distance ($\text{Na}_2\text{HPO}_4 \cdot 12\text{H}_2\text{O}$).

If we compare the results of the analytical solution with experimental measuring of those materials [4], we can see a good agreement.

3. Mathematical and Numerical Model

The thermal model is derived in detail in [6]. The mathematical model of air velocity distribution uses fluid equations which were derived for incompressible fluid with the condition (for the detailed description see [5])

$$\text{div } \mathbf{v} = 0 \quad (17)$$

for a steady state of flow holds the continuity equation

$$\text{div } \rho \mathbf{v} = 0 \quad (18)$$

We assume a turbulent flow

$$\text{rot } \mathbf{v} = 2\boldsymbol{\omega} \quad (19)$$

where $\boldsymbol{\omega}$ is the angular velocity of fluid. If we use the Stokes theorem, the Helmholtz theorem for moving particle and continuity equation, we can formulate from the equilibrium of forces the Navier-Stokes equation for the fluid element [11]

$$\frac{\partial \mathbf{v}}{\partial t} + (\text{grad } \mathbf{v}) \cdot \mathbf{v}^T = \mathbf{A} - \frac{1}{\rho} \text{grad } p + \mathbf{v} \cdot \Delta \mathbf{v} \quad (20)$$

where \mathbf{A} is the external acceleration and \mathbf{v} the vector of kinematic viscosity and $(grad \mathbf{v})$ has the dimension of tensor. In the equation (20) we substitute pressure losses

$$\begin{aligned} grad p = & - \left(K_x \rho v_x |\mathbf{v}| + \frac{f}{D_h} \rho v_x |\mathbf{v}| + C_x \mu v_x \right) \mathbf{u}_x - \\ & - \left(K_y \rho v_y |\mathbf{v}| + \frac{f}{D_h} \rho v_y |\mathbf{v}| + C_y \mu v_y \right) \mathbf{u}_y - \\ & - \left(K_z \rho v_z |\mathbf{v}| + \frac{f}{D_h} \rho v_z |\mathbf{v}| + C_z \mu v_z \right) \mathbf{u}_z \end{aligned} \quad (21)$$

where K are the suppressed pressure losses, f the resistance coefficient, D_h the hydraulic diameter of ribs, C the air permeability of system, μ the dynamic viscosity and \mathbf{u} the unit vector of the Cartesian coordinate system. The resistance coefficient is got from the Boussinesq theorem

$$f = aRe^{-b} \quad (22)$$

where Re is Reynolds number and a, b are the coefficients from [14]. The model of short deformation field is formulated from the condition of steady-state stability, which is expressed

$$\int_{\Omega} \mathbf{f} d\Omega + \int \mathbf{t} d\Gamma = 0 \quad (23)$$

where \mathbf{f} are the specific forces in the domain Ω , and \mathbf{t} pressures, tensions and shear stresses on the interface area Γ . By means of the transformation into local coordinates we obtain the differential form for the static equilibrium

$$\mathbf{f} + div^2 \mathbf{T}_v = 0 \quad (24)$$

where div^2 states for div operator of tensor quantity and \mathbf{T}_v is the tensor of internal tension

$$\mathbf{T}_v = \begin{bmatrix} X_x & X_y & X_z \\ Y_x & Y_y & Y_z \\ Z_x & Z_y & Z_z \end{bmatrix} \quad (25)$$

where X, Y, Z are the stress components which act on the elements of the area. It is possible to add a form of specific force from (17)-(20) to the condition of static equilibrium. The form of specific force is obtained by means of an external acceleration \mathbf{A} , on the condition that pressure losses and shear stresses τ are given as

$$\rho \left(\frac{\partial \mathbf{v}}{\partial t} + (\mathbf{grad} \mathbf{v}) \cdot \mathbf{v}^T \right) - \rho \mathbf{A} - \sum_{l=1}^{N_s} \mathbf{F}_l + div^2 \mathbf{T}_v = \boldsymbol{\theta} \quad (26)$$

where \mathbf{F}_l are the discrete forces and div^2 is the divergence operator of tensor. The model, which covers the forces, viscosity, and pressure losses is

$$\begin{aligned} \rho \left(\frac{\partial \mathbf{v}}{\partial t} + (\mathbf{grad} \mathbf{v}) \cdot \mathbf{v}^T \right) - \rho \mathbf{A} - \sum_{l=1}^{N_s} \mathbf{F}_l + \\ + grad p - \mu \cdot \Delta \mathbf{v} = 0. \end{aligned} \quad (27)$$

We can prepare the discretization of equation (20) by means of the approximating of velocity \mathbf{v} and acceleration \mathbf{a}

$$\begin{aligned} \mathbf{v} = \sum_{k=1}^{N_\phi} \mathbf{v}_{vk} W_k(x, y, z), \quad \forall (x, y, z) \in \Omega, \\ \mathbf{a} = \sum_{k=1}^{N_\phi} \mathbf{a}_{vk} W_k(x, y, z), \quad \forall (x, y, z) \in \Omega, \end{aligned} \quad (28)$$

where $\mathbf{v}_v, \mathbf{a}_v$ are the instantaneous node values, W is the base function, N_ϕ is the number of mesh nodes. If we apply the approximation (26) and the Galerkin principle in (27), we get the semidiscrete solution and after another rewriting we obtain the model of air flow

$$\begin{aligned} \rho \int_{\Omega} W_j W_i d\Omega \frac{d\mathbf{v}_{vi}}{dt} + \\ + \rho \int_{\Omega} W_j \mathbf{v}_{vi} \cdot \left(\frac{dW_i}{dx} \mathbf{u}_x + \dots + \frac{dW_i}{dz} \mathbf{u}_z \right) d\Omega \mathbf{v}_{vi} + \\ + \int_{\Omega} W_j \cdot \left(\frac{dW_i}{dx} \mathbf{u}_x + \dots + \frac{dW_i}{dz} \mathbf{u}_z \right) d\Omega p_i - \\ - \rho \int_{\Omega} W_j d\Omega \mathbf{A}_i - \int_{\Omega} W_j d\Omega \mathbf{F}_{li} - \\ - \int_{\Omega} \left(\frac{dW_j}{dx} + \frac{dW_j}{dy} + \frac{dW_j}{dz} \right) \mathbf{v}_i \cdot \\ \cdot \left(\frac{dW_i}{dx} \mathbf{u}_x + \frac{dW_i}{dy} \mathbf{u}_y + \frac{dW_i}{dz} \mathbf{u}_z \right) d\Omega \mathbf{v}_{vi} - \\ - \int_{\Gamma} W_j d\Gamma \mathbf{X}_i = 0, \quad i, j = 1, 2, \dots, N_v. \end{aligned} \quad (29)$$

On the interface there are boundary conditions formulated

$$\mathbf{n} \cdot (\mathbf{v}) = 0 \quad (30)$$

on the border Γ_{air} where \mathbf{n} is a normal vector to the direction of air flow

$$\mathbf{n} \cdot (p) = 0 \quad (31)$$

on the border Γ_{Cu} where $\Gamma_{air} \subset \Gamma_{Cu}$ is the interface between the solid body and air. The boundary conditions for thermal model are

$$\mathbf{n} \times (grad T) = 0, \quad \text{on } \Gamma_{air} \cup \Gamma_{PCM} \quad (32)$$

and the initial conditions

$$T(x, y, z, t)|_{t=0} = T_{0,air} = T_{0,PCM}, \quad \text{on } \Gamma_{air} \cup \Gamma_{PCM} \quad (33)$$

$$T(x, y, z, t)|_{t=0} = T_{0,Cu}, \quad \text{on } \Gamma_{Cu} \quad (34)$$

The initial conditions for the air flow in the domain Ω are

$$v_{0,air}(z, t)|_{t=0} = 0, 1 \text{ m.s}^{-1}. \quad (35)$$

$$p_{0,air}(t)|_{t=0} = 10 \text{ Pa}, \quad (36)$$

out of the domain Ω is the air velocity and pressure null.

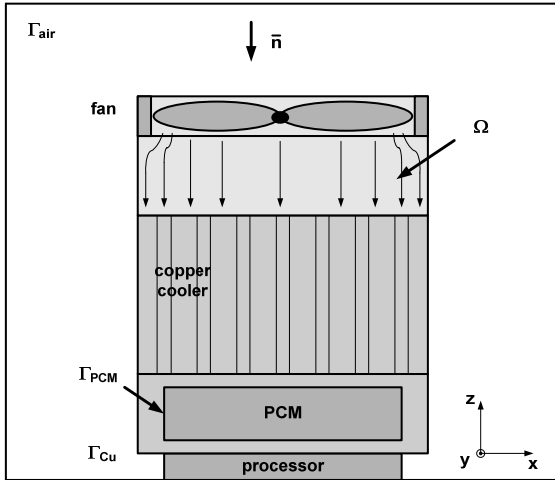


Fig. 9. Geometric model of Cu-cooler with mesh of elements.

We can write the form for an element of mesh

$$\begin{aligned} & \left[C_e^f \right] \left\{ \frac{dv_{vi}}{dt} \right\} + \left[K_e^{sx} - K_e^{Fx} \right] \{ v_{vi} \} + \left[K_e^{cx} \right] p_i = \\ & = \left[K_e^{gx} \right] \{ A_i \} + \left[F_e^{bx} \right] \{ F_{ii} \} + \left[F_e^{sx} \right] \{ X_i \} \end{aligned} \quad (37)$$

$e = 1, 2, \dots, N_e$.

Matrixes C_{ij}^f , K_{ij}^{sx} , K_{ij}^{Fx} , K_{ij}^{cx} , K_{ij}^{gx} , F_{ij}^{bx} , K_{ij}^{Fx} , F_{ij}^{sx} are related to coefficients of equations (29).

For the solution we used the SST model (Shear Stress Transport Model) which is offered by the commercial software ANSYS FLOTTRAN. The SST model combines and switches between $k-\epsilon$ and $k-\omega$ model automatically in order to get the best result (see [2], [7], [10]). The $k-\epsilon$ model gives good results in the distance from walls and $k-\omega$ is more exact near walls. For the description of different turbulent models you can see [12], [13], [14].

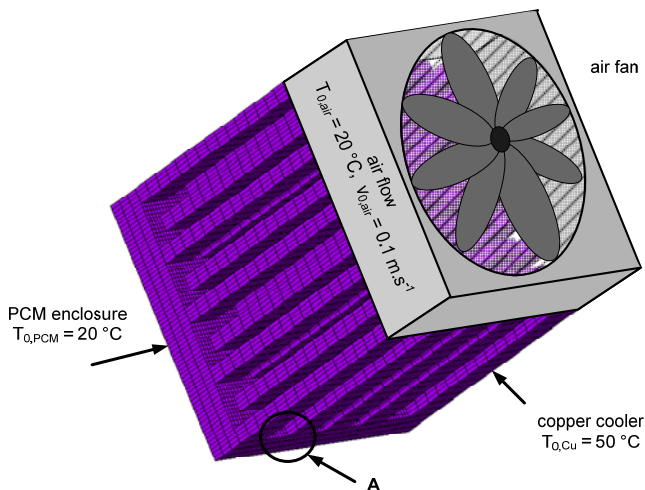


Fig. 10. Geometric model of Cu-cooler with mesh of elements.

The progress of numerical solution consists of two parts. Firstly, we solve the turbulence model and get heat transfer coefficients on the surface of ribs. Those results are the input of the second part when the thermal model is calcu-

lated. We obtain the time dependence of temperature distribution in PCM. There is the geometric model of copper cooler in Fig.10. The $\text{CaCl}_2 \cdot 6\text{H}_2\text{O}$ is closed inside of the bottom plate (see Fig. 2). The size of the plate is $30 \times 30 \times 5$ mm and the ribs are 20 mm high. The PCM volume is about $3,8 \cdot 10^{-6} \text{ m}^3$. The plate takes heat from the processor up and crystalline salt starts to melt at T_m . The air flows through ribs and extracts heat from the cooler.

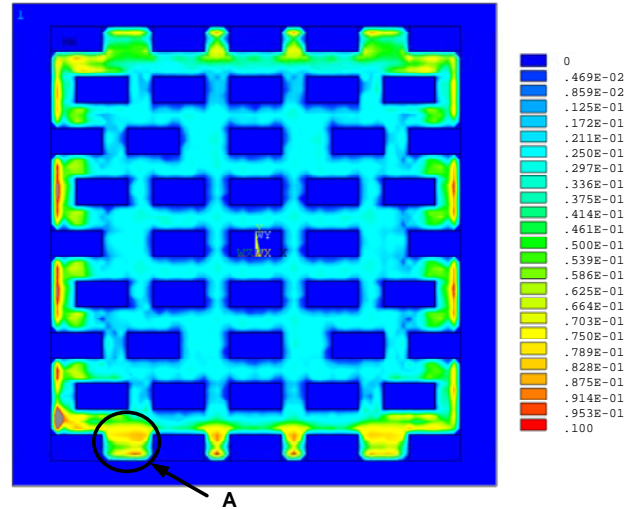


Fig. 11. The distribution of air velocity module.

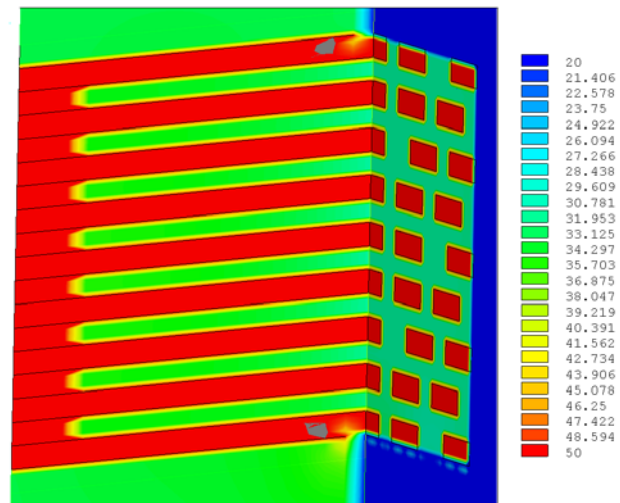


Fig. 12. Temperature distribution in the cooler (the cross section).

In Fig. 11 there is the distribution of air velocity module. We can see the effective rise of air flow velocity on the bottom of ribs (the detail A in Fig. 10, 11). Temperature distribution in ribs is shown in Fig. 12. Fig. 13 compares the results of numerical simulation with the measuring in the middle of PCM enclosure. We measured the temperature by means of the probe. The differences between the simulation and the measuring are due to the inaccuracy of the model with respect to reality. We used tabular values of pure $\text{CaCl}_2 \cdot 6\text{H}_2\text{O}$ but we modified hexahydrate with 1,2% of BaCO_3 in order to avoid supercooling and deformations of cooling curves after more cycles of melting and freez-

ing. In order to obtain exact results, we would need to know the temperature dependence of thermal conductivity, specific heat, and density during the phase change (see [8]).

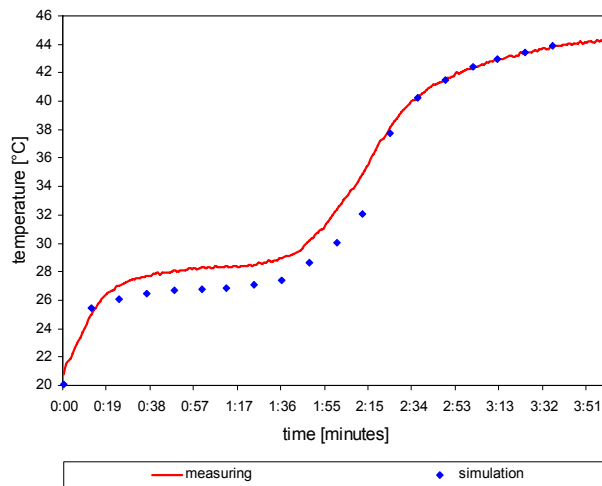


Fig. 13. Time dependence of temperature in $\text{CaCl}_2 \cdot 6\text{H}_2\text{O}$.

4. Conclusion

This paper deals with the application of phase change materials for thermal management of integrated circuits. We presented analytical description and solution of heat transfer and phase change in 1D and also mathematical and numerical model of air turbulence. The model of the real 3D copper cooler was solved by means of FEM in ANSYS software. We computed the problem of air flow turbulence, heat transfer, heat conduction and convection, and also phase change. If we compare the results of simulation with the experimental measuring, we see the good agreement. The exact knowledge of material properties has the crucial effect on the accuracy of the numerical model.

Acknowledgements

The paper was prepared within the framework of the research plan No. MSM 0021630516 of the Ministry of Education, Youth and Sports of the Czech Republic.

References

- [1] ADAM, J. Wärme- und Kühlmanagement in elektronischen Geräten. *Elektronik Praxis*, 2007, vol. 3, p. 74-76.
- [2] *Ansys User's Manual*. Huston (USA): SVANSON ANALYSYS SYSTEM, Inc., 1994-2006.
- [3] ARSLANTÜRK, C. Small-time analytical solution of phase change problems in cylindrical and spherical domains. *Journal of Thermal Sciences and Technology*, 2004.

- [4] BĚHUNEK, I. Properties of inorganic PCM. In *Honeywell EMI conference and competition 2005*. Brno (Czech Republic), 2005. ISBN 80-214-2942-9.
- [5] FIALA, P. *Induction Flowmeter Model DN-100* (research report). UTEE FEKT VUT, Brno, 2001 (in Czech).
- [6] FIALA, P. *Transformer Short Test Modeling*. PhD thesis. UTEE FEKT VUT, Brno, 1998 (in Czech).
- [7] KOZEL, K. *Numerical Solution Methods of Flow Problems I*. Prague: ČVUT Publishing (in Czech).
- [8] LAMBERG, P., LEHTINIEMI, R., HENELL, A-M. Numerical and experimental investigation of melting and freezing in phase change material storage. *Applied Mathematical Modelling* 32, 2004.
- [9] LANE, G.A. *Solar Heat Storage: Latent Heat Materials, Volume II: Technology*. Boca Raton (Florida, USA): CRC Press, Inc., 1986.
- [10] ŘÍHA, J. *Hydrodynamic and Dispersive Effects Mathematical Modeling*. Brno: VUT Publishing, 1997 (in Czech). ISBN 80-214-0827-8.
- [11] SPECHT, B. *Modellierung von beheizten laminaren und turbulenten Strömungen in Kanälen beliebigen Querschnitts*. Braunschweig (Germany): Technische Universität Carolo-Wilhelmina, 2000.
- [12] PISZACHICH, W. S. *Nonlinear Models of Flow, Diffusion and Turbulence*. Leipzig (Germany): Teubner Verlagsgesellschaft, 1985.
- [13] WILCOX, D.C. *Turbulence Modeling for CFD*. La Canada (California, USA): DCW Industries, Inc., 1994.
- [14] ZHANG, Y. *Finite Elemente zur Berechnung instationärer Strömungen mit bewegten Wandungen*. Stuttgart (Germany): Universität Stuttgart, 1996.

About Authors...

Ivo BĚHUNEK was born in Jihlava in 1979. In 2002 he obtained M.Sc. degree in Electrical Power Engineering at the Brno University of Technology. He finished and defended his dissertation (Ph.D.) at the same university in 2005. Dr. Běhunek is a member of the IEE.

Pavel FIALA (* 1964 in Kraslice) received Ing. (M.Sc.) and Dr. (Ph.D.) degrees from the Brno University of Technology (BUT), Faculty of Electrical Engineering and Communication (FEEC) in 1988 and 1998, respectively. Since 1998 he has been with the Dept. of Theoretical and Experimental Electrical Engineering of FEEC BUT as the assistant professor and associate professor (since 2005). He occupies the position of the head of department.

Dr. Fiala has authored or co-authored more than 60 papers in scientific journals and conference proceedings. His research has been focused on numerical modeling and optimization of coupled electromagnetic, thermal, and mechanical systems. He deals with the design and development of high power pulse sources and devices for neutralizing anti-personnel mines (Ministry of Defense, PROTOTYP A). He cooperates with ABB very closely. Mr. Fiala works within the framework of the European research project WISE – research and development of sensors for aviation and astronautics (EADS, DASSAULT AVIATION, Eurocopter, TELETELL). Dr. Fiala is a member of the SPIE, APS, IEEE, IEE, OSA.